JOC The Journal of Organic Chemistry

Article

pubs.acs.org/joc

Degenerate Molecular Shuttles with Flexible and Rigid Spacers

D. Deniz Günbaş and Albert M. Brouwer*

Van't Hoff Institute for Molecular Sciences, University of Amsterdam, P.O. Box 94157, 1090 GD Amsterdam, The Netherlands

Supporting Information

ABSTRACT: The preparation and dynamic behavior of degenerate rotaxane molecular shuttles are described in which a benzylic amide macrocycle moves back and forth between two naphthalimide-glycine units along a diphenylethyne spacer or an aliphatic spacer consisting of a C_9, C_{12}, or C_{26} alkyl chain. Subtle differences in the ^{1}H NMR spectra of the rotaxanes can be related to the presence of conformers in which the macrocycle interacts simultaneously with both glycines, especially in the case of the C_9 spacer. The kinetic data of the shuttling behavior in the C_{26} rotaxane were obtained from dynamic NMR spectroscopy. The Eyring activation parameters were found to be $\Delta H^{\ddagger} = 10 \pm 1$ kcal mol^{-1}, $\Delta S^{\ddagger} = -6.5 \pm 2.0$ cal mol^{-1} K^{-1}, $\Delta G^{\ddagger}_{298} = 11.9 \pm 0.2$ kcal mol^{-1}. For the systems with the shorter spacers, the shuttling rates were higher. Also in the diphenylethyne, rotaxane shuttling is rapid on the NMR time scale, indicating that the rigid unit does not impose a large barrier to the translocation of the macrocycle.

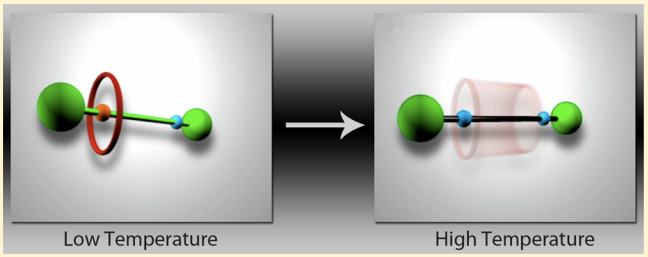

INTRODUCTION

Molecular shuttles[1−5] based on [2]rotaxanes[6−16] that have two recognition sites for the moving macrocyclic ring have attracted much attention due to their applications in molecular switches[17−19] and molecular machines.[20−29] One of the key features of such systems is the control of the shuttling movement of the ring along the dumbbell component, which is mainly affected by the noncovalent binding interactions between the two components. Many bistable [2]rotaxanes have been designed in such a way that two translational isomers are created, which are populated in a particular ratio depending primarily on the relative strengths of the interactions between the macrocycle and the two stations.[11,30−32] In such systems, external stimuli may be used to switch between the states defined by the position of the macrocyclic ring.[1,8,33]

In most of our previous work in this field, we have studied rotaxanes containing a succinamide or related diamide binding motif, in combination with imides as photoactive units and tetralactam macrocycles as moving beads.[8,9,34−40] Such diamides are effective templates for the synthesis of rotaxanes in a five-component clipping reaction.[41] More recently, we introduced a glycine unit next to the naphthalimide, in order to influence the energy landscape of the molecular shuttle. This resulted in a distribution of coconformers in which the macrocycle does not encircle the succinamide station exclusively but also resides over the *ni-gly* station to a significant extent.[42] The *ni-gly* station, however, clearly is a weaker binding site for the ring than the succinamide. Therefore, on the basis of the common assumption that breaking of the hydrogen bonds with the station is the rate-limiting step,[8,35] we expect that shuttling can be faster in rotaxanes containing only *ni-gly* units. Here we present one approach that involves constructing degenerate [2]rotaxanes in which both recognition sites positioned along the thread are identical, so that the shuttling process between two isoenergetic forms can be simply observed by dynamic ^{1}H NMR spectroscopy.[2,5,31,43−45] By taking into account that the macrocycle must pass over the spacer units to move back and forth between the two recognition sites, the shuttling speed can be influenced by incorporating spacer units with different length and volume into the degenerate [2]rotaxanes. Here we will describe (1) the preparation and characterization of degenerate [2] rotaxanes (**1**−**4**, shown in Figure 1, and their corresponding dumbbell components, **5**−**8**) having flexible alkane or rigid unsaturated spacers in between their two *ni-gly* stations, and (2) dynamic ^{1}H NMR experiments in order to study the shuttling rates and to analyze the magnitude of the shuttling barrier of the benzylic amide macrocycle in the degenerate rotaxane **3**.

RESULTS

Rotaxanes with Flexible Spacers. The routes employed in the synthesis of the degenerate, two station [2]rotaxanes containing flexible spacers **1**−**3** and their corresponding dumbbell-shaped compounds **5**−**7** are outlined in Scheme 1. We chose to keep the nature of the diamine the same in all three cases. However, the length of the spacer unit was varied from a short C_9 alkyl chain via an intermediate-length C_{12} to a long C_{26} spacer. Threads **5** and **6** were obtained in 65 and 60% yields, respectively, by a coupling reaction of 2 equiv of the carboxylic acid derivative **9**, which was synthesized following a literature procedure,[46] with commercially available 1,9-diaminononane **10** and 1,12-diaminododecane **11**, respectively, in the presence of benzotriazole-1-yl-oxy-tris-(dimethylamino)-

Received: May 4, 2012
Published: June 4, 2012

   dx.doi.org/10.1021/jo300907r | J. Org. Chem. 2012, 77, 5724−5735

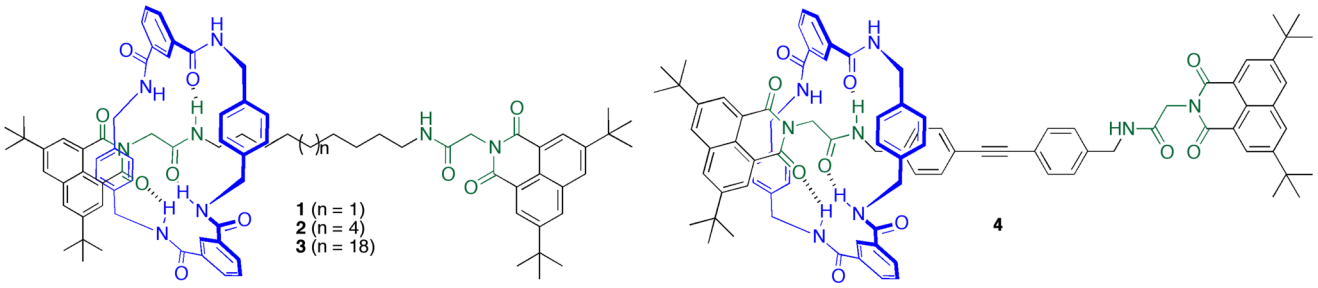

Figure 1. Structures of degenerate [2]rotaxanes containing flexible (**1**–**3**) and rigid (**4**) spacers.

Scheme 1[a]

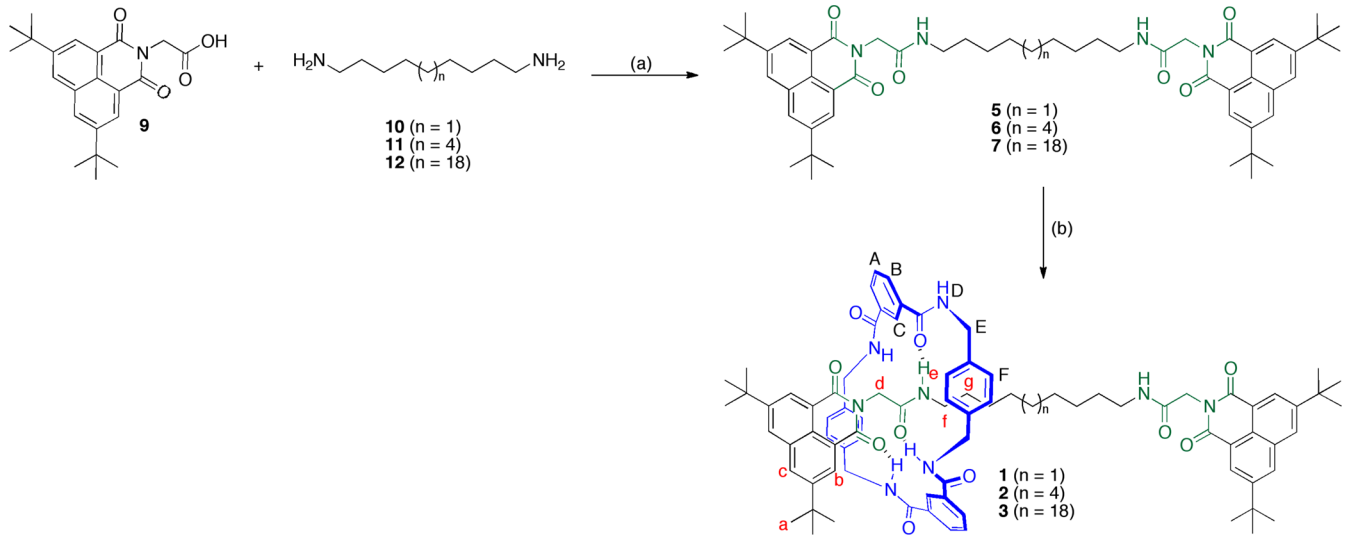

[a](a) 1,9-Diaminononane **10** (n = 1), 1,12-diaminododecane **11** (n = 4), or 1,26-diaminohexacosane **12** (n = 18), BOP, DIPEA, DMF, rt, 20 h, 65, 60, and 62%, respectively. (b) Isophthaloyl dichloride, p-xylylene diamine, Et_3N, $CHCl_3$, rt, 20 h, 7, 8, and 7%, respectively.

phosphonium hexafluorophosphate (BOP) and diisopropylethylamine (DIPEA) in DMF at room temperature. Similarly, naphthalimide-containing thread **7** was prepared in 62% yield from the reaction of compound **9** with 1,26-diaminohexacosane **12**, synthesized using a previously described procedure.[47]

Treatment of threads **5**–**7** with 12 equiv of isophtaloyl dichloride and p-xylylenediamine (Et_3N, $CHCl_3$) afforded the desired rotaxanes **1**–**3**, which were isolated after column chromatography on silica gel in 7, 8, and 7%, yields, respectively, as analytically pure white solids. The unreacted threads **5**–**7** were recovered.

As shown in Figures 2, 3, and 4, at room temperature in $CDCl_3$ rotaxanes **1**–**3** exhibit the ^{1}H NMR spectra of compounds possessing 2-fold symmetry, leading to the appearance of only one set of signals for the protons of stoppers and stations. The signals of the macrocycle methylene groups (H_E, see Scheme 1) appear as a singlet, indicating rapid exchange of the pseudoequatorial and pseudoaxial protons. This implies that the macrocycle rapidly shuttles between two degenerate hydrogen-bonding (*ni-gly*) stations and also "pirouetting" around the thread is fast.[39]

In C_9-rotaxane **1**, glycine protons (H_d) are shielded by the p-xylylene rings of the macrocycle and experience significant shifts when compared to thread **5** ($\Delta\delta_{obs}$ = −0.41 ppm). The chemical shift observed is the average of that of the methylene group that is shielded by the macrocycle and the other one at the other side of the molecule, which is in an environment that

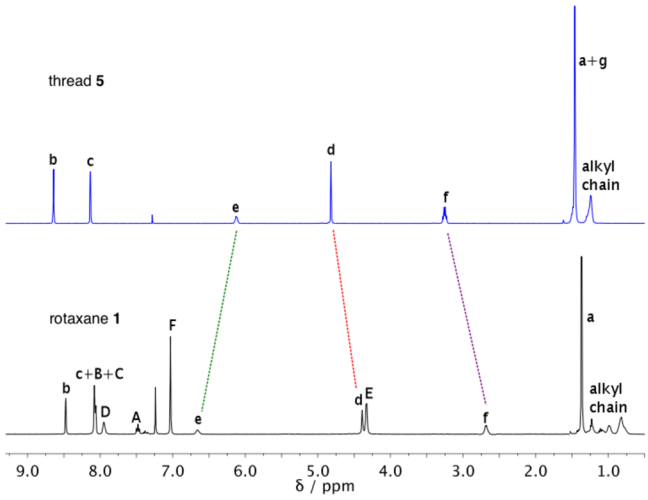

Figure 2. ^{1}H NMR spectra of C_9-thread **5** and rotaxane **1** (400 MHz, $CDCl_3$, 298 K). For labels, see Scheme 1.

is similar to that in the thread. Thus, the intrinsic shielding of the methylene group at which the ring is located must be twice this amount: $\Delta\delta_{shielding}$ = −0.82 ppm. The signals centered at 2.93 ppm for the H_f protons are also shifted downfield compared to those in free dumbbell component **5**: $\Delta\delta_{shielding}$ = −0.61 ppm. This clearly indicates that they are also located in the vicinity of the macrocyclic ring. Moreover, the signals

dx.doi.org/10.1021/jo300907r | J. Org. Chem. 2012, 77, 5724–5735

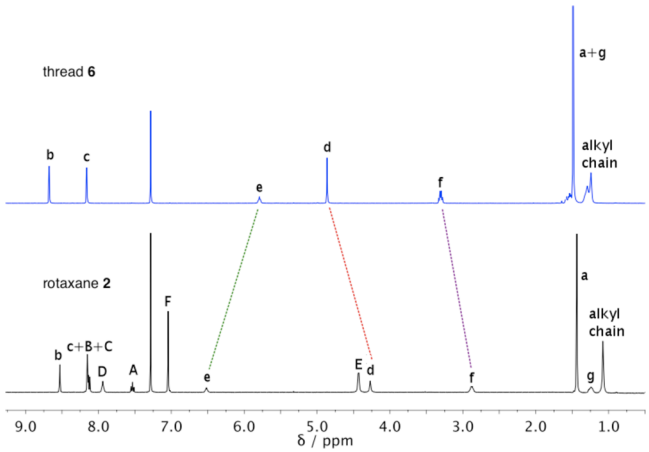

Figure 3. ^{1}H NMR spectra of C_{12}-thread **6** and rotaxane **2** (400 MHz, $CDCl_3$, 298 K). For labels, see Scheme 1.

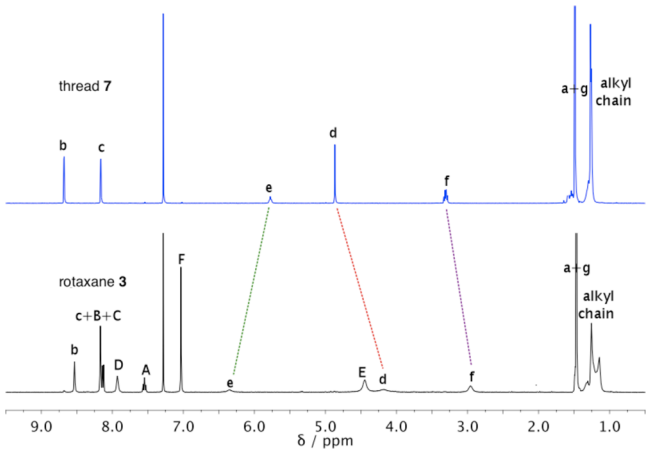

Figure 4. ^{1}H NMR spectra of thread **7** and rotaxane **3** (400 MHz, $CDCl_3$, 298 K). For labels, see Scheme 1.

assigned to amide protons (H_e) underwent significant downfield shift ($\Delta\delta_{obs}$ = 0.53 ppm), which strongly implies their involvement in hydrogen-bonding interactions with the macrocycle. Apart from this, the signals corresponding to the alkyl chain were shielded by up to 0.46 ppm suggesting that the macrocyclic ring also spends an appreciable time on the aliphatic spacer, possibly in bridged or folded coconformations (see below).

In C_{12}-rotaxane **2**, the ^{1}H NMR signals corresponding to the glycine protons (H_d) experience a significant upfield shift of $\Delta\delta_{shielding}$ = −1.18 ppm[42] with respect to those of thread **6**, which is considerably larger than what was found for rotaxane **1**. Furthermore, the methylene groups adjacent to the glycine-NH's (H_f) were shielded ($\Delta\delta_{shielding}$ = −0.43 ppm) but less than in rotaxane **1**. On the other hand, amide protons (H_e) were significantly shifted downfield ($\Delta\delta_{obs}$ = 0.73 ppm), which is more than in rotaxane **1**. In addition, the CH_2 protons of the aliphatic spacer display only slight shielding. All these features indicate that in rotaxane **2**, which has a slightly longer spacer than rotaxane **1**, the macrocyclic ring is held more tightly to the naphthalimide unit, and the population of bridged or folded coconformers is small.

In the case of C_{26}-rotaxane **3**, localization of the macrocycle over the *ni-gly* stations is even more pronounced than in **2**. The glycine signal shows an upfield shift ($\Delta\delta_{shielding}$ = −1.36 ppm) compared to its positions in thread **7**, somewhat larger than in rotaxane **2**. In addition, smaller shielding for the H_f protons ($\Delta\delta_{shielding}$ = −0.35 ppm) further support the idea that the ring component resides predominantly next to the naphthalimide unit. The amide protons (H_e) underwent downfield shifts by 0.57 ppm with respect to those of the corresponding thread, which is less than in rotaxane **2**. It is noteworthy that the signals in the ^{1}H NMR spectrum of rotaxane **3** are broader than in thread **7**.

While the NMR spectra of rotaxanes **1**, **2**, and **3** all indicate that the macrocyclic ring is hydrogen-bonded to the glycine unit(s), the differences in the shielding patterns are significant. In **3**, in which the probability of an interaction between the two ends of the molecule is the smallest, the shielding of the CH_2 protons next to the imide (H_d) is the strongest, while that of the first CH_2 group of the alkane spacer (H_f) is the smallest. Moreover, shielding of other methylene groups of the spacer is negligible in **3**, small in **2**, but substantial in **1**. In the discussion of the structures of rotaxane molecular shuttles, the focus is on the coconformations, but this gives only a part of the picture. Even when the macrocyclic ring encircles a glycine unit, it can adopt numerous local energy minima. Moreover, when the flexible backbone is appropriately folded, the macrocycle can interact with the other station through one of its amide groups that is not interacting with the encircled station. Figure 5 gives an example of a possible structure for a "folded" *ni-gly* coconformer of the C_9 rotaxane **1**.

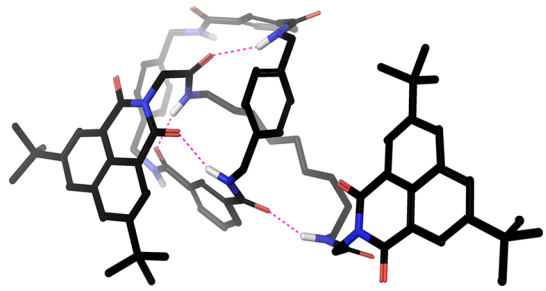

Figure 5. Snapshot from an MD simulation of rotaxane **1** illustrating the position of the macrocycle on the thread with an intercomponent hydrogen bonding motif in a folded coconformer.

In such a structure, the ring is pulled away from the *ni*-unit, and consequently, less shielding of H_d and stronger shielding of H_f and other methylene groups can be expected. Another possibility would be that the ring binds equally strongly to both stations and resides in the middle of the thread.[48] Attempts to generate models of such structures in molecular dynamics simulations of **1** were not successful: the system always evolved to folded structures similar to that shown in Figure 5. It is well-known that alkane coconformers can be obtained in DMSO, which disrupts the hydrogen bonds and induces shielding of the alkane by the macrocyclic ring due to solvophobic effects.[49] Of the rotaxanes discussed here, only **2** and **3** were soluble in DMSO. The spectra are shown in Figures 6 and 7. Evidently, much stronger shielding of the middle part of the thread is observed than in **1** in $CDCl_3$. Moreover, the methylene groups (H_d) of the *ni-gly* unit are not shielded.

Rotaxane with a Rigid Spacer. Rotaxanes containing flexible spacers such as **1** can adopt many different conformations in solution, which makes it impossible to define the structures precisely. Introduction of rigidity into the rod

dx.doi.org/10.1021/jo300907r | J. Org. Chem. 2012, 77, 5724−5735

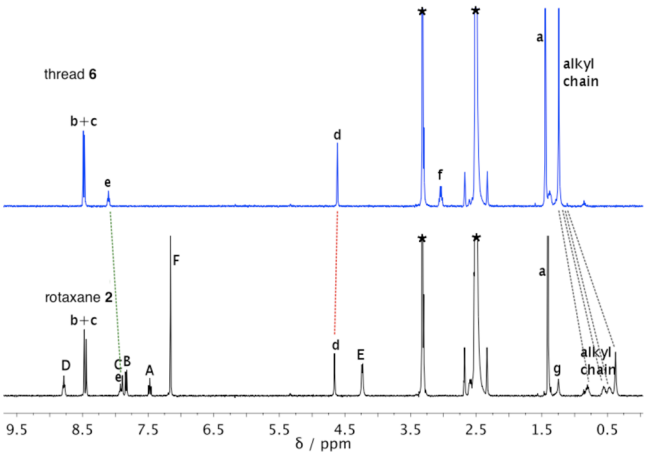

Figure 6. ^{1}H NMR spectra of C_{12}-thread **6** and rotaxane **2** in DMSO-d_6 (400 MHz, 298 K). The assignments correspond to those indicated in Scheme 1. The residual peaks of solvent and H_2O are marked with asterisks (*).

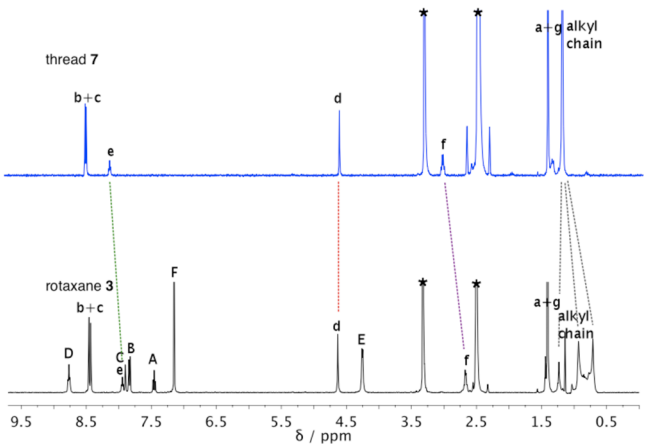

Figure 7. ^{1}H NMR spectra of C_{26}-thread **7** and rotaxane **3** in DMSO-d_6 (400 MHz, 298 K). The assignments correspond to those indicated in Scheme 1. The peaks of the residual solvent and H_2O are marked with asterisks (*).

component of degenerate molecular shuttles limits the number of geometries that can be adopted, which allows the design of molecular machines and switches with better control of the submolecular motion.[50] Moreover, back-folding[51] in bistable [2]rotaxanes can be prevented by replacing the flexible linkers with linear rigid ones. This is particularly important for the fabrication of surface-based machinery.[52] Consequently, creating rigidified rotaxanes provides well-defined structures and motions, which is a significant advantage over flexible ones.

Here we describe rotaxane **4** with a rigid diphenylethyne spacer as a bridge between two *ni-gly* stations. Rotaxane **4** was synthesized as outlined in Scheme 2.

Initially, the HCl salt of 4-iodobenzylamine **13** was transformed in 75% yield into *N*-Boc 4-iodobenzylamine **14** using a modification of the method described by Lee et al.[46] A Pd-catalyzed Sonogashira cross coupling reaction of the amine-protected iodide **14** with trimethylsilyl (TMS) acetylene gave the TMS-protected compound **15** (90%), and a subsequent desilylation with tetrabutylammonium fluoride (TBAF) provided the 4-acetylenebenzylamine **16** (98%).[46] The synthesis of compound **17** was accomplished by a Pd-catalyzed cross coupling reaction between **16** and **14** in 85% yield, and the following removal of the Boc protection group afforded **18** in 98% yield. Coupling of **18** with **9** resulted in the formation of the desired thread **8** in 90% yield. Rotaxane **4** was obtained in 6% yield by applying the same protocol as described for **1**−**3**.

Only one set of signals is observed for both stoppers and stations in the ^{1}H NMR spectrum at 298 K (Figure 8), from which we conclude that the macrocycle undergoes a fast exchange between the two binding sites. The signals assigned to H_d protons exhibit a significant upfield shift with $\Delta\delta_{shielding}$= −1.43 ppm with respect to their positions in the corresponding thread **8**. The H_f protons are shifted by $\Delta\delta_{shielding}$= −0.64 ppm. In addition, the downfield shift of the amide protons (H_e, from δ = 6.11 ppm to δ = 6.58 ppm) in rotaxane **4**, implies that they are also a part of the hydrogen-bonding interactions with the macrocycle. Interaction between the macrocycle and the diphenylethyne unit is apparent from the shielding of H_g and H_h. The extent of deshielding of H_e and shielding of H_f protons, respectively, in rotaxane **4** are smaller than in rotaxanes **1**−**3**. Together with the stronger shielding of H_d, this indicates that the macrocycle in the equilibrium structure is relatively close to the imide due to steric hindrance of the phenyl rings in the thread.

Dynamic NMR Spectroscopy. Since the switching rates of bistable [2]rotaxanes are important performance indicators for molecular shuttles, we performed NMR experiments at variable temperatures in order to provide more information regarding the kinetic parameters of the shuttling process. The thread components **5**−**8** of rotaxanes **1**−**4** are symmetric and consist of two equivalent halves. Localization of the ring on one of the two possible recognition sites breaks this symmetry. If the ring shuttles back and forth between these two degenerate forms rapidly on the ^{1}H NMR time scale, then it will appear as if the 2-fold symmetry has been restored.

As the temperature is decreased, this shuttling process becomes slow on the ^{1}H NMR time scale and ultimately, at a low enough temperature, the symmetry will be broken, and the signals in the ^{1}H NMR spectrum separate into pairs of equal intensity signals. One set corresponds to the stopper nearby the recognition site where the macrocycle is located and the other to the more distant stopper. At intermediate temperatures, line broadening and coalescence of the signals can be expected.[53]

The temperature dependence of the ^{1}H NMR spectrum of degenerate rotaxanes **1** and **2** in $CDCl_3$ was studied in the range 253−328 K. Rotaxane **3** (Figure 9) could be investigated over the temperature range 218−328 K. For rotaxanes **1** and **2**, the spectra below 253 K could not be recorded because of a loss of homogeneity of the samples. In the case of rotaxane **3**, temperatures below 218 K were not reachable as the compound crystallized in the NMR tube. ^{1}H NMR peak shapes for rotaxane **3** as a function of temperature are shown in Figures 10 and 11. The related spectra for rotaxanes **1** and **2** are shown in the Supporting Information and in ref 42, respectively. Lowering the temperature did not lead to significant changes in the ^{1}H NMR spectra of **1** and **2** except for some broadening of the signals and increased deshielding of the amide protons. In marked contrast, lowering the temperature in the case of **3** in $CDCl_3$ led to the anticipated splitting of the signals into pairs. Figure 10 shows the ^{1}H NMR spectra of rotaxane **3** in the range 7−9 ppm. The signal corresponding to H_b protons, which appears at 8.52 ppm at 328 K splits into two signals, at 8.64 and 8.21 ppm at 218 K. Likewise, the peak assigned to H_c protons, which resonates at 8.14 ppm at 328 K, is split into two signals at 8.32 and 8.16 ppm. The signals observed at 8.64 and

dx.doi.org/10.1021/jo300907r | J. Org. Chem. 2012, 77, 5724−5735

Scheme 2[a]

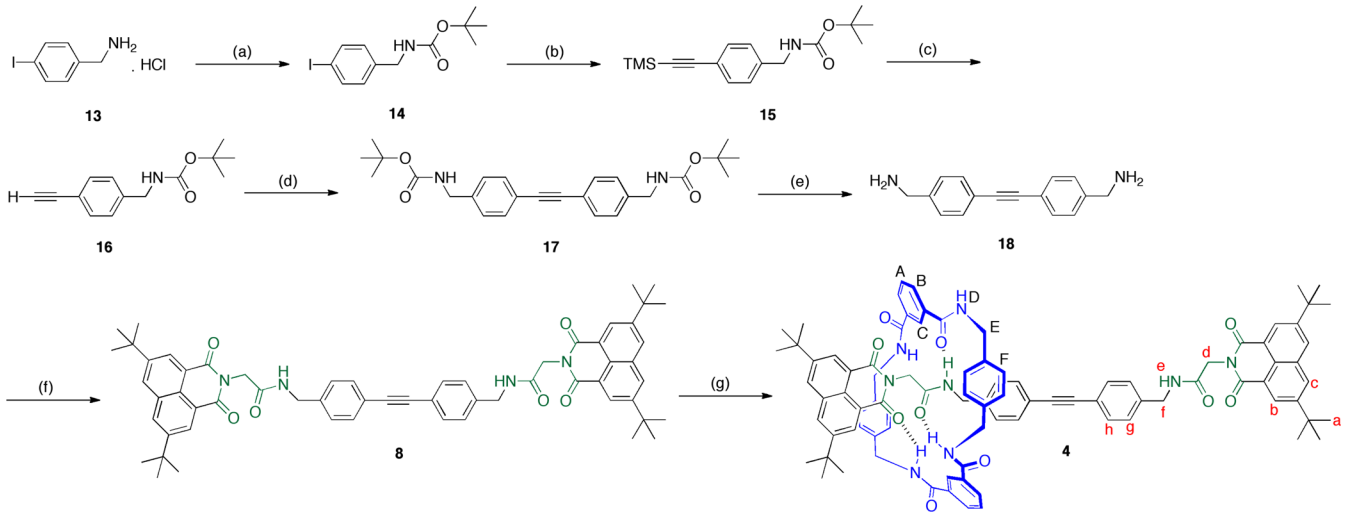

[a](a) Di-*tert*-butyl dicarbonate, Et_3N, THF, rt, overnight, 75%. (b) (Trimethylsilyl)acetylene, $(PPh_3)Pd_2Cl_2$, CuI, THF, 50 °C, 2 h, 90%. (c) TBAF, CH_2Cl_2, rt, 1 h, 98%. (d) Compound **14**, $(PPh_3)Pd_2Cl_2$, CuI, toluene, 60 °C, 1 day, 85%. (e) TFA, CH_2Cl_2, 0 °C, 1 h, 98%. (f) Compound **9**, BOP, DIPEA, DMF, rt, overnight, 90%. (g) Isophthaloyl dichloride, *p*-xylylene diamine, Et_3N, $CHCl_3$, rt, 20 h, 6%.

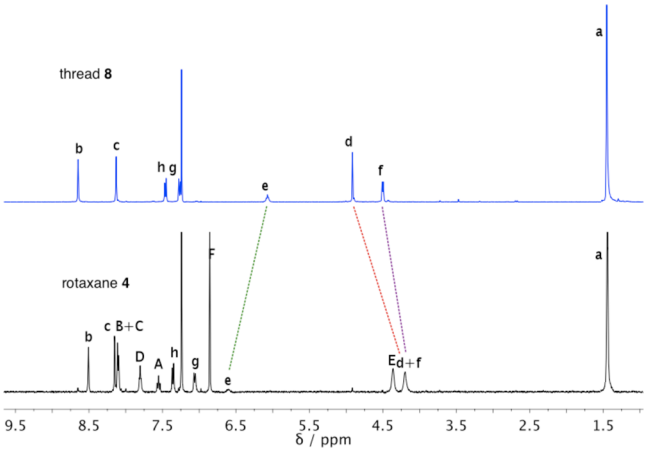

Figure 8. ^{1}H NMR spectra of thread **8** and rotaxane **4** (400 MHz, $CDCl_3$, 298 K). Assignments correspond to the labels in Scheme 2.

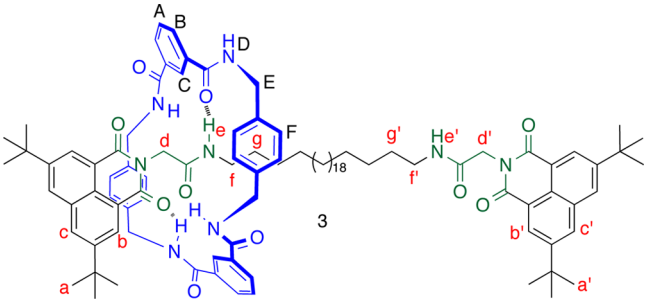

Figure 9. Atom numbering for nondegenerate coconformer of rotaxane **3**.

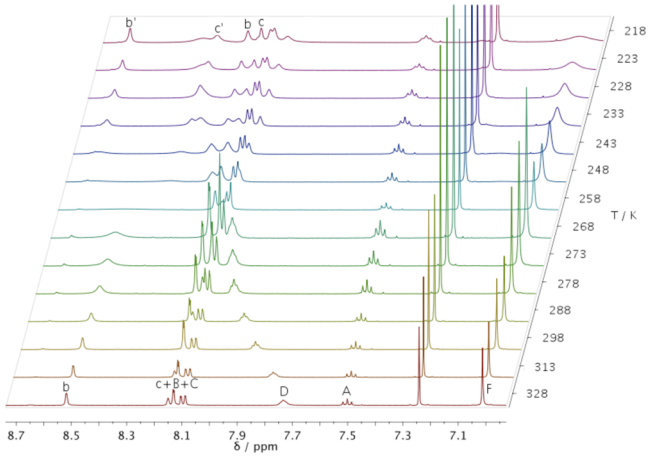

Figure 10. Section of the variable temperature ^{1}H NMR spectra (500 MHz, $CDCl_3$) of rotaxane **3**. The assignments correspond to the labeling in Figure 9.

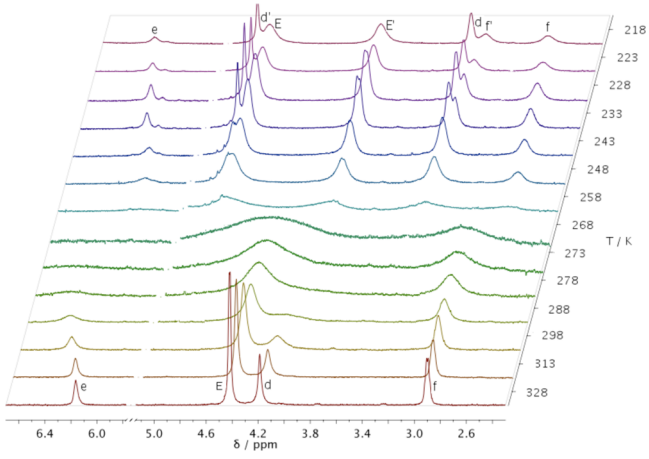

Figure 11. Sections of the variable temperature ^{1}H NMR spectra (500 MHz, $CDCl_3$) of rotaxane **3**. The assignments correspond to the labeling in Figure 9.

8.16 ppm at 218 K correspond to $H_{b'}$ and $H_{c'}$, which are opposite to the macrocycle and in good accordance with the peaks associated with H_b and H_c protons in the corresponding thread **8**. Furthermore, as depicted in Figures 10 and 11, lower temperatures caused significant shifts of the H_D and H_e to higher frequencies. This is not surprising as the strength of

dx.doi.org/10.1021/jo300907r | J. Org. Chem. 2012, 77, 5724−5735

noncovalent hydrogen-bonding interactions becomes stronger with a decrease in temperature.

Remarkably, at low temperature the signal of the *p*-xylylene protons H_F shows a strong broadening, indicating the onset of a decoalescence. This probably means that rotation of these aromatic rings about their C_1-C_4 axis is restricted.[40]

At room temperature, the methylene protons of the macrocycle (H_E) resonate as a broad singlet at 4.43 ppm (Figure 4). At 248 K and below, rotaxane **3** shows clearly separate signals of H_E protons at 4.85 ppm and $H_{E'}$ at 4.01 ppm (values at 218 K). The signals of H_E and $H_{E'}$ belong to the methylene protons on different sides of the macrocyclic ring, one facing the naphthalimide, the other facing the thread. The protons of the glycine CH_2 (H_d) appear at 4.2 ppm at 328 K and split into two signals at 4.95 and 3.31 ppm at 218 K. In addition, at 328 K, the H_f protons of rotaxane **3** resonate at 2.90 ppm, while at low temperatures, two signals were observable at 3.19 and 2.72 ppm for $H_{f'}$ and H_f protons, respectively. These findings clearly show that the shuttling is slow on the NMR time scale at low temperatures. The protons H_d and H_f are strongly shielded by the aromatic ring currents of the macrocycle, and the signals of $H_{d'}$ and $H_{f'}$ appear at almost the same chemical shift values as in the thread **8** (4.89 and 3.25 ppm, respectively, at room temperature).

Apart from these, at lower temperatures the signals corresponding to H_e protons underwent a significant downfield shift due to the increasing strength of hydrogen-bonding interactions with the macrocycle. The peaks associated with H_d and H_f protons undergo coalescences at temperatures (T_c) of 258 and 268 K, respectively.

An estimation of the rate of the shuttling process was obtained using the coalescence method. This method is optimally applied to an equally populated two-site system formed by uncoupled nuclei, with a chemical shift difference ($\Delta\nu$) much greater than the line width in the absence of exchange, and undergoing exchange with a rate constant ($k_1 = k_{-1}$) that is larger than the intrinsic transverse relaxation time. For such a system, below and up to coalescence, there is a simple relationship between the observed separation of the two peaks ($\Delta\nu_e$) and the rate constant.[54]

$$k = \frac{\pi}{\sqrt{2}}(\Delta\nu^2 - \Delta\nu_e^2)^{1/2} \tag{1}$$

Although eq 1 could be used to extract the rate constants, it does not give very accurate results because the experimental frequency difference is not very sensitive to changes in k. Moreover, in the temperature range 223–248 K, peaks of H_d and $H_{f'}$ and of H_E and $H_{d'}$ overlap, which makes it difficult to determine the $\Delta\nu$ values accurately. At coalescence ($\Delta\nu_e = 0$), eq 1 simplifies to a well-known expression:

$$k_1 = k_{-1} = k = \frac{\pi\Delta\nu}{\sqrt{2}} = \frac{\pi(\nu_A - \nu_B)}{\sqrt{2}} \tag{2}$$

Use of eq 2 requires knowing $\Delta\nu$, which is the frequency difference between the exchanging peaks obtained by measurements at lower temperatures, at slow exchange.

The free energy of activation $\Delta G^{\ddagger}$ for the exchange can be directly calculated from the coalescence temperature (T_c) using the Eyring equation (eq 3):

$$\Delta G^{\ddagger} = -RT_c \ln\left(\frac{kh}{k_B T_c}\right) \tag{3}$$

where R is the gas constant, h is Planck's constant, k_B is the Boltzmann constant, T_c is the coalescence temperature, and k is the rate constant of exchange (s^{-1}).

The kinetic parameters obtained from the coalescence temperature of the ^{1}H NMR spectra for the dynamic process observed in rotaxane **3** are listed in Table 1. A free energy of activation ($\Delta G^{\ddagger}$ = 11.6 kcal mol^{-1}) was calculated at the coalescence temperature (T_c = 268 K) using the frequency difference ($\Delta\nu$ = 820 Hz) for H_d and $H_{d'}$ protons according to the above relationship. Similarly, H_f and H_b protons were used leading to $\Delta G^{\ddagger}$ values of 11.8 and 11.9 kcal mol^{-1}, respectively.

Table 1. Kinetic and Thermodynamic Parameters[a] for the Shuttling Behavior of the Macrocyclic Ring between Two *nigly* Stations in Rotaxane 3 Using the Coalescence Method[b]

probe H	T_c (K)	$\Delta\nu$ (Hz)	k (s^{-1})[c]	$\Delta G^{\ddagger}$ (kcal mol^{-1})[d]
H_d	268	820	1822	11.6
H_f	258	235	522	11.8
H_b	258	215	478	11.9

[a] ^{1}H NMR spectra recorded at 500 MHz in $CDCl_3$ solution. [b] T_c = coalescence temperature, $\Delta\nu$ = limiting chemical shift difference, k = rate constant. [c] Estimated error ±10 s^{-1}. [d] Estimated error ±0.2 kcal mol^{-1}.

To decompose the activation free energy into enthalpic and entropic terms by means of the Eyring equation, the rates have to be measured over a range of temperatures. This sometimes can be accomplished by determining the coalescence temperatures of several pairs of the sites that are affected by the same chemical process, but have different $\Delta\nu$ values, and therefore different coalescence temperatures. The most accurate results are obtained using complete line shape analysis.[55] In this approach, experimental shapes are compared with those calculated using sets of kinetic and spectroscopic parameters until the agreement is reached for a set of temperatures. The application of the latter technique in the present case was hampered by the fact that the signals of the probe protons overlap with each other or with other protons at several temperatures studied.

At $T > T_c$, the fast exchange regime, the situation can be treated very simply by invoking the uncertainty principle. If the lifetime of a nucleus in environment A is τ_A, then the uncertainty in the energy is $\Delta U = \hbar\tau_A^{-1}$. This will influence directly the widths of the relevant NMR lines.[53] For the case of simple (uncoupled) two-site exchange, A ⇄ B, with equal populations, a single Lorentzian line is observed with a line width given by the following eq 4:

$$\Delta\nu_{1/2} = \frac{1}{2}\pi(\nu_A - \nu_B)^2 k^{-1} \tag{4}$$

Also in this regime of exchange, information on k can only be obtained from the line width if the chemical shift difference ($\nu_A - \nu_B$) is known.

The estimated rates of shuttling are listed in Table 2 using the observed $\Delta\nu$ (Table 1) and $\Delta\nu_{1/2}$ obtained at different temperatures. As the data in Table 2 reveal, the rate constants decrease upon cooling, and the values obtained for two different probe protons are in a reasonable agreement with each other. Fitting to the Eyring equation (Figure 12) gave the activation parameters $\Delta H^{\ddagger}$ = 10 ± 1 kcal mol^{-1} and $\Delta S^{\ddagger}$ = −6.5 ± 2.0 cal mol^{-1} K^{-1}.

dx.doi.org/10.1021/jo300907r | J. Org. Chem. 2012, 77, 5724–5735

Table 2. Bandwidth at Half Maximum Intensity of the Exchange-Broadened Signal ($\Delta\nu_{1/2}$)[a] and Rates (k)[b] Estimated According to eq 4 for H_d and H_b Protons at Various Temperatures

	H_d		H_b	
temperature	$\Delta\nu_{1/2}$ (Hz)	$k \times 10^4$ (s^{-1})	$\Delta\nu_{1/2}$ (Hz)	$k \times 10^4$ (s^{-1})
328	14	7.5	2.6	2.8
313	26	4.0	2.8	2.6
298	85	1.3	3.2	2.2
288	184	0.57	5.9	1.2
278	nd[c]	nd[c]	13	0.57
273	nd[c]	nd[c]	20	0.37
268	nd[c]	nd[c]	32	0.22

[a]Values are obtained from the data at $T > T_c$, corrected for the line width in the absence of exchange (~1.0 Hz) estimated from the residual solvent peaks. [b]Value ± 0.1 × 10^4 (s^{-1}). [c]Value could not be determined.

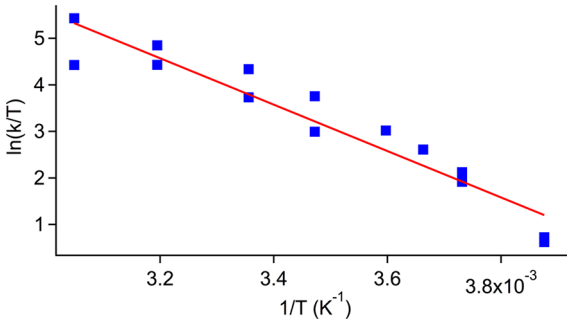

Figure 12. Eyring plot created from the data in Tables 1 and 2 for the degenerate rotaxane **3** containing a flexible C_{26} linker. The values for $\Delta H^{\ddagger}$ = 10 ± 1 kcal mol^{-1} and $\Delta S^{\ddagger}$ = −6.5 ± 2.0 cal mol^{-1} K^{-1} were obtained from the slope and intercept of the plot, respectively.

Solvent Effects. Inspired by these results, we decided to investigate the influence of solvent polarity on the shuttling barrier in rotaxane **3**. The kinetic behavior was examined in acetone-d_6, which is expected to weaken the noncovalent hydrogen-bonding interactions since it is more polar and a better hydrogen-bond acceptor than $CDCl_3$. As illustrated in Figure 13, comparison of the ^{1}H NMR spectra of rotaxane **3** and the corresponding thread **7** recorded in acetone-d_6 at room temperature revealed that signals associated with H_d protons are shifted upfield ($\Delta\delta_{shielding}$ = −0.53 ppm) but much less than in $CDCl_3$ ($\Delta\delta_{shielding}$ = −1.36 ppm). The reduced differential chemical shift of H_d protons presumably stems from diminishing of hydrogen-bonding interactions between the macrocycle and the thread as a result of competing interactions with the solvent molecules. The chemical shifts of the protons (H_e) in thread **7** (δ = 7.41 ppm) are larger than in rotaxane **3** (δ = 7.28 ppm), which suggests that the solvent is a more effective hydrogen-bond acceptor than the macrocyclic ring in rotaxane **3**. On the other hand, observed shielding of the alkyl chain by as much as 0.56 ppm with respect to their positions in thread **7** indicates that the macrocycle not only resides over the *ni-gly* station but is also positioned over the alkyl chain to some extent. Weakening of the hydrogen-bonding interactions between the macrocycle and the thread with polar acetone-d_6 leads to unsatisfied hydrogen-bonding interactions between the two components. As a result, the rotaxane may adopt a folded conformation so that the amides at both ends of the thread can reach the macrocyclic binding sites. Notably, strong shielding of

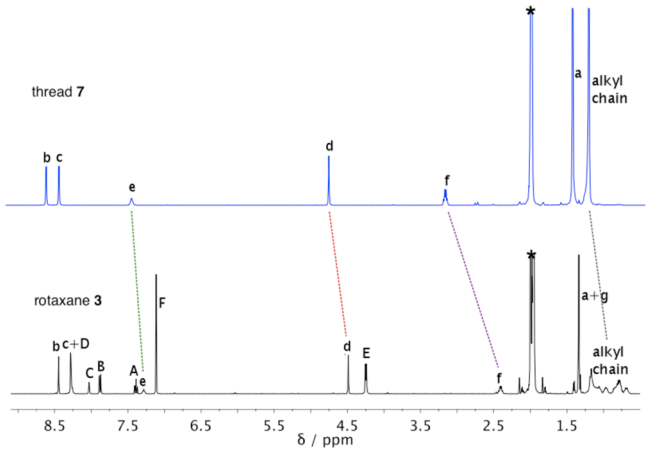

Figure 13. ^{1}H NMR spectra of thread **7** and rotaxane **3** (400 MHz, acetone-d_6, 298 K). Lettering corresponds to the labels shown in Scheme 1. The peaks of the residual solvent are marked with asterisks (*).

H_f protons ($\Delta\delta$ = −0.78 ppm) further confirms that the ring is loosely bound to the *ni-gly* station. Because of the weaker intercomponent interactions, the macrocycle moves around where the space is available, i.e., less near the naphthalimide, more near the alkyl chain. Another possibility is that rotaxane **3** in acetone-d_6 exists to some extent as an alkane coconformer in which the ring is detached from both stations.

Rotating frame Overhauser effect spectroscopy (ROESY) NMR analysis of rotaxane **3** in acetone-d_6 shows that the benzylic amide macrocycle protons (H_C, H_D, H_E, H_F) have through space correlations to CH_2 protons of the aliphatic spacer of the thread (Figure 14). Such correlations were not observed in $CDCl_3$.

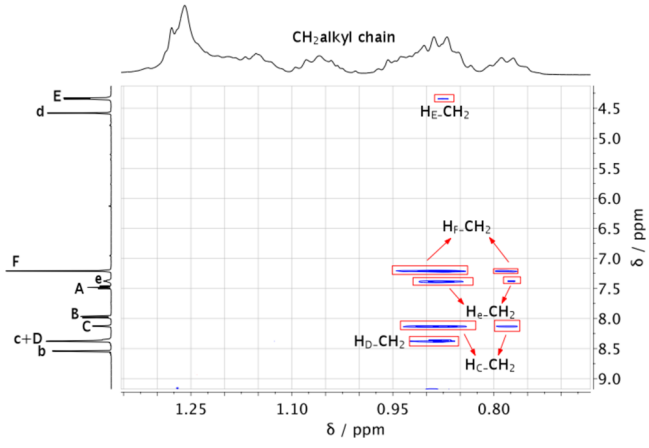

Figure 14. Partial ROESY NMR spectrum of **3** in acetone-d_6 at 298 K (400 MHz).

The influence of the temperature on the ^{1}H NMR spectra of rotaxane **3** in acetone-d_6 was studied at temperatures in the range 243−318 K (Figures 15 and 16). The two stations appeared as one set of signals and did not exhibit peak splitting at low temperatures. As shown in Figure 15, lowering the temperature leads to a significant shift of the amide protons (H_D and H_e) to higher frequencies, whereas the positions of aromatic protons were affected insignificantly. The protons of the glycine unit (H_d) (Figure 16) are deshielded as the

dx.doi.org/10.1021/jo300907r | J. Org. Chem. 2012, 77, 5724−5735

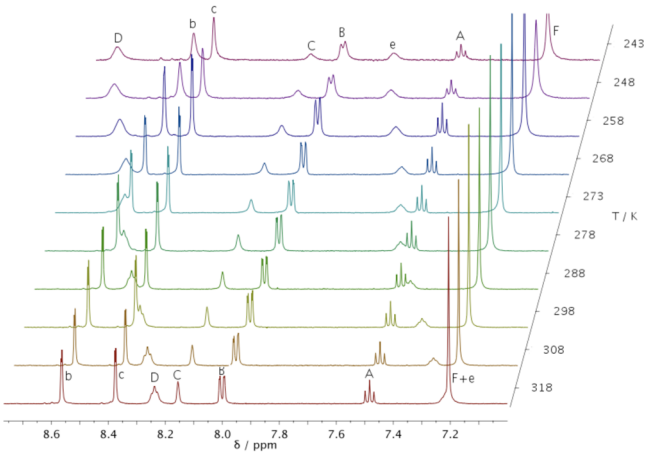

Figure 15. Signals of aromatic ring protons in the variable temperature ^{1}H NMR spectra (500 MHz, acetone-d_6) of rotaxane **3**.

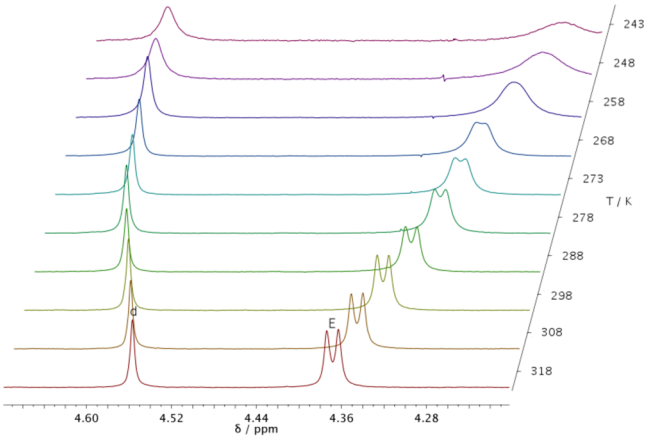

Figure 16. Signals of H_d and H_E in the variable temperature ^{1}H NMR spectra (500 MHz, acetone-d_6) of rotaxane **3**.

temperature is decreased, which could arise from the increasing amount of folded or alkane coconformers with a decrease in temperature. The protons of the central part of the thread are indeed somewhat more shielded at lower temperatures (not shown). No coalescence was observed for H_d protons within the temperature range 243−318 K, but the signals associated with H_E protons begin to decoalesce at 248 K (Figure 16). Unfortunately, the low solubility of the rotaxane at lower temperatures did not allow us to observe the full dynamic behavior: line broadening, coalescence, and final line narrowing. Comparison of the results with those obtained above, however, clearly shows that the coalescence temperatures are substantially lower in acetone-d_6 than in $CDCl_3$.

Similarly, it was attempted to investigate the barrier for the movement of the macrocycle along the rigid diphenylethyne spacer in rotaxane **4** by acquiring ^{1}H NMR spectra at a variety of different temperatures in $CDCl_3$. The compound was quite soluble in $CDCl_3$ at room temperature, and a well-resolved spectrum was obtained. Upon cooling, the peaks undergo a significant line broadening, but this is partly due to loss of homogeneity resulting from poor solubility of **4** at lower temperatures. We note, however, that in contrast to the case of **3**, no line broadening is observed in the NMR spectra of **4** at room temperature, indicating more rapid exchange in **4**.

DISCUSSION

Systematic investigation and efficient control of the dynamic processes are prerequisites for the future application of rotaxanes as molecular devices. Although noncovalent interactions in a variety of [2]rotaxane systems has been extensively investigated, there have been only few systematic studies of the distance dependence of the shuttling rate in hydrogen-bond-based rotaxanes.

The chemical shifts of the methylene groups surrounding the glycine stations (H_d and H_f) and those of the alkane chain give valuable information on the molecular structure of the rotaxanes **1**−**4**. In $CDCl_3$ at 298 K, clear trends are visible in the series C_9−C_{12}−C_{26}: the shielding of H_d increases, the shielding of H_f decreases, and the shielding of the other methylene groups in the alkane spacer decreases. The relative shieldings of H_d and H_f give information on the location of the ring around the glycine station: when H_d is more shielded (and H_f less), it is on average closer to the imide; when H_d is less shielded (and H_f more), the ring is closer to the alkane spacer. We propose that in the C_9 rotaxane **1**, the ring is pulled toward the alkane chain by a hydrogen bond between the ring and the distant glycine, as shown in Figure 5. Infrared studies of the related naphthalimide/succinamide rotaxanes have indicated that such coconformers can exist also there, in particular in the reduced form, in which the ring hydrogen bonds to the naphthalimide anion and can have a remote interaction with the succinamide station.[38,56] In the C_{12} rotaxane **2** such bridging interactions are less important than in **1**, and in the C_{26} rotaxane **3** they are even less significant for statistical reasons.

Whereas DMSO completely disrupts the binding between the macrocycle and the glycine units in rotaxanes **2** and **3**, the moderately hydrogen bond accepting solvent acetone has a more complex effect. Compared to the situation in chloroform, we observe less shielding of H_d and more shielding of H_f relative to the thread **7**. This indicates that the ring is closer to the methylene protons of the central part of the thread, which are also shielded, and show through-space interactions with the macrocycle protons in a ROESY experiment. Possibly coconformations with the macrocycle bound to the glycines coexist with "alkane" coconformers.

The finding of bridged structures may be important for the understanding of the shuttling mechanism in rotaxanes of this type. In recent work of Panman et al., it was shown that the rather steep distance dependence of the rate of shuttling in photoreduced naphthalimide/succinamide rotaxanes can be described with a biased random walk model, which is based on the assumption that the ring is detached from the succinamide station and moves toward the reduced naphthalimide in a random walk.[8,35] Alternatively, if the transition state of the reaction involves simultaneous hydrogen bonding of the ring with both stations, this may also explain why the reaction is relatively faster for shorter spacers. Application of the distance dependence observed by Panman to the present systems would lead us to predict that the rates for the C_{12} rotaxane and the C_9 rotaxane compared to the C_{26} system are 30 and 66 times faster, respectively. Such a rate difference is compatible with the observation of fast exchange at $T > 268$ K. Of course, it is possible that the precise mechanism of molecular shuttling changes with chain length, solvent, and/or temperature.

In the rotaxane **4** with the rigid spacer, the macrocycle is more tightly bound to the glycine unit than in **3**. Yet, rapid shuttling occurs at room temperature, indicating that the

dx.doi.org/10.1021/jo300907r | J. Org. Chem. 2012, 77, 5724−5735

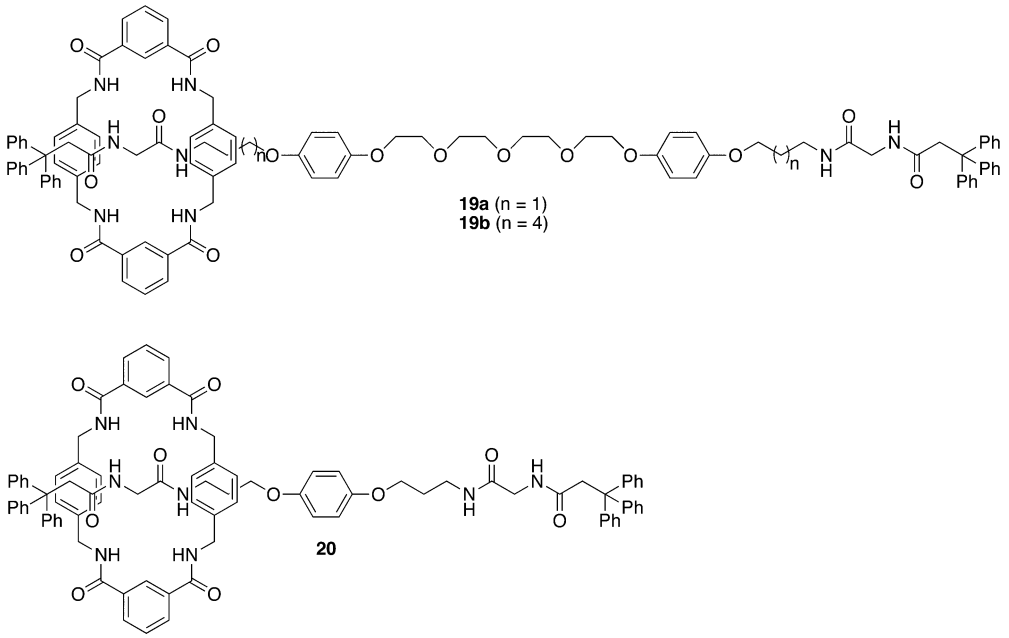

Figure 17. Chemical structures of rotaxanes **19a**, **19b**, and **20** containing different lengths of spacers.[5]

diphenylethyne unit does not form a serious barrier to the translational motion. Unfortunately, kinetic parameters could not be obtained for this system because of a lack of solubility.

As a chemical approach to control the rate of shuttling, Zhao et al. reported [2]rotaxane systems **19a**, **19b**, and **20** shown in Figure 17.[5] The $\Delta G^{\ddagger}$ values of **19a** and **19b** (11.5 and 11.7 kcal mol^{-1}, respectively) are comparable to our results in with the C_{26} rotaxane **3**, implying that the hydroquinone unit incorporated between the hydrogen-bonding stations in rotaxanes **19a** and **19b** does not impose an important barrier on the shuttling.

Also in the rigid rotaxane **4** it appears that spacers of this size do not substantially hinder shuttling. Clearly, once the hydrogen bonding of the macrocycle to an individual station is broken, the distance it must travel to the next station is much more influential on the rate of shuttling than steric barriers that are not large enough to completely prevent the passage of the macrocycle. Molecular mechanics calculations give a distance of 3.1 nm between the two *ni-gly* stations in the extended conformation of rotaxane **3**, whereas it is 3.2 and 3.9 nm, respectively, for rotaxanes **19a** and **19b**. On the other hand, for [2]rotaxane **20** the shuttling was too fast to be detected within the temperature range investigated. This closely resembles the situation observed in the case of rotaxane **1** and **2** containing relatively shorter alkyl chains (C_9 and C_{12}) in our work.

In addition, Leigh and co-workers reported that combining two (or more) hydrogen-bonding peptide units with a hydrocarbon or thioether gave a $\Delta G^{\ddagger}$ for shuttling of 11.2 ± 0.3 kcal mol^{-1} for **21a**, 12.4 ± 0.3 kcal mol^{-1} for **21b**, and 10.9 ± 0.3 kcal mol^{-1} for **21c**, respectively at 298 K (Figure 18).[2] The molecular structure reveals a distance between the two stations of 1.6, 2.5, and 1.5 nm for **21a**, **21b**, and **21c**, respectively. The increased activation energy cost (1.2 kcal mol^{-1}) for **21b** over **21a** was attributed to the increased distance that the macrocycle must travel between the peptide stations. Moreover, the free energy of activation in **21b** is of the same order of magnitude as in rotaxane **3**, which has a distance of 3.1 nm between the two degenerate *ni-gly* stations.

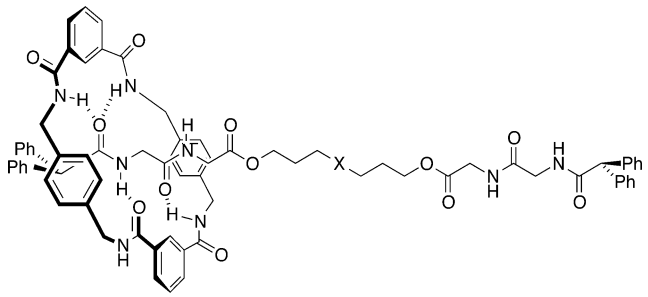

Figure 18. Structure of peptide-based molecular shuttles **21a** (X = $(CH_2)_2$), **21b** (X = $(CH_2)_{10}$), and **21c** (X = S).[2]

The papers of Zhao et al. and of Lane et al., only reported $\Delta G^{\ddagger}$ values at fixed temperatures. For the shuttling in rotaxane **3** we have determined the enthalpy and entropy of activation as $\Delta H^{\ddagger}$ = 10 ± 1 kcal mol^{-1} and $\Delta S^{\ddagger}$ = −6.5 ± 2.0 cal mol^{-1} K^{-1}. Negative values of the activation entropy for molecular shuttles have also been observed in the naphthalimide/succinamide systems studied earlier in our laboratory.[8,36] This may be related to a low probability of success of the biased random walk proposed by Panman et al.[34,35] Alternatively, if shuttling occurs via bridged conformations, it may be attributed to a combination of low probability of reaching such conformations and the constrained structure of the interlocked assembly in the transition state.

■ CONCLUSIONS

The synthesis and characterization of degenerate molecular shuttles containing flexible and rigid spacers (**1**–**3** and **4**, respectively) has been reported. Variable temperature NMR spectroscopy was performed to obtain kinetic data for shuttling of the benzylic amide macrocycle between two *ni-gly* stations by making the path along either a rigid diphenylethyne unit or a flexible aliphatic spacer (C_9, C_{12}, C_{26}). These kinds of degenerate molecular shuttles can serve as models to investigate the barriers to ring displacement in the nondegenerate molecular bistable [2]rotaxanes employed in electronic devices.

dx.doi.org/10.1021/jo300907r | J. Org. Chem. 2012, 77, 5724−5735

The shuttling kinetics in rotaxane **3** in $CDCl_3$ were determined using dynamic NMR measurements. Enthalpic and entropic values were derived from an Eyring plot, which led to $\Delta H^{\ddagger} = 10 \pm 1$ kcal mol^{-1} and $\Delta S^{\ddagger} = -6.5 \pm 2.0$ cal mol^{-1} K^{-1}.

In acetone-d_6, somewhat surprisingly, folded or alkane coconformers of **3** appear to be populated next to those in which the macrocycle is bound to the glycine units. Although broadening of the signals was observed at lower temperatures, the insufficient solubility of **3** in this solvent prevented the determination of the shuttling kinetics. The same limitation was encountered in the case of rotaxane **4** containing a rigid spacer. The absence of line broadening in the NMR spectra of **4** at room temperature shows that the shuttling rate is higher than in **3**. Thus, the rigid diphenylethyne unit does not form a high barrier for the shuttling of the macrocycle between the two degenerate sites.

EXPERIMENTAL SECTION

Materials. All glassware, stirrer bars, syringes, and needles were either oven- or flame-dried prior to use. All reagents, unless otherwise indicated, were obtained from commercial sources. Anhydrous THF was obtained by distillation from Na/Ph_2CO under Ar. The reactions were carried out under N_2 or Ar atmosphere. Melting points were determined on a Reichert apparatus and are uncorrected. Rotaxane **2** and thread **6** were available from earlier work.[42] 2-(Acetic acid)-5,8-di-*tert*-butyl-benzo[de]isoquinoline-1,3-dione **9**,[57] hexacosane-1,26-diamine **12**, and *tert*-butyl-4-ethynylbenzylcarbamate **16**[46] were prepared according to procedures reported in the literature.

Methods. Stochastic dynamics calculations were carried out using MacroModel, version 9.9 (Schrödinger, LLC, New York, NY, 2012), with the AMBER* force field and the GBSA solvent model for chloroform. Most ^{1}H and ^{13}C were recorded at 25 °C on a 9.4 T spectrometer (400 and 100 MHz, respectively). Chemical shifts are in parts per million (ppm) using either the solvent's residual protons or TMS employed as the internal standard. Coupling constants (J) are reported in hertz (Hz). ROESY data were recorded using the following acquisition parameters: data points = 2048, relaxation delay = 2 s, mixing time = 200 ms. Processing parameters: size = 2048 × 2048, window function = sine. Variable temperature NMR spectra were recorded on a 500 MHz spectrometer. Multiplicities are given as s (singlet), d (doublet), dd (doublet of doublets), t (triplet), m (multiplet), and b (broad). Fast atom bombardment (FAB) mass spectra were obtained using a four-sector mass spectrometer comprising magnetic and electrostatic mass analyzers, equipped with a Xenon primary atom beam, utilizing a 3-nitrobenzoyl alcohol (3-NOBA) matrix. Microanalyses were performed by an independent external service provider. Other abbreviations used: Et_2O = diethylether, MeOH = methanol, EtOAc = ethyl acetate, TFA = trifluoroacetic acid, Et_3N = triethylamine, BOP = benzotriazole-1-yl-oxy-tris-(dimethylamino)-phosphonium hexafluorophosphate, DIPEA = *N*,*N*-diisopropylethylamine, TBAF = tetrabutylammonium fluoride, $(PPh_3)Pd_2Cl_2$ = dichlorobis(triphenylphosphine)palladium(II), CuI = copper(I) iodide.

General Procedure for Rotaxane Synthesis. The thread and Et_3N (24 equiv) were dissolved in chloroform (75 mL) and stirred vigorously, while solutions of the *p*-xylylene diamine (12 equiv) and isophthaloyl dichloride (12 equiv) in $CHCl_3$ (20 mL) were simultaneously added over a period of 4 h using a motor-driven syringe pump. The resulting suspension was stirred overnight, filtered through a pad of Celite to remove any polymeric material, and concentrated. The crude product was column chromatographed to yield, in order of elution, the unconsumed thread and the corresponding rotaxane.

General Procedure for Pd-Catalyzed Coupling Reaction. The iodo and ethynyl substrates and the Pd reagents in THF were placed in a Schlenk flask, which was evacuated and purged with argon three times. The argon flow rate was increased, the threaded stopcock was removed, and Et_3N was added in a succession by gastight syringe. The threaded stopcock was replaced, the argon flow rate was reduced, and the Schlenk flask was immersed in an oil bath held at constant temperature. When the reaction was finished, the flask was cooled to room temperature, and the solvents were removed under reduced pressure. To remove Pd species, the mixture generally was filtered through a short silica column.

[2]-(1,4,7,14,17,20-Hexaaza-2,6,15,19-tetraoxo-3,5,9,12,16,18,22,25-tetrabenzocyclohexacosane)-*N*,*N*′-(nonane-1,9-diyl)bis(2-(5,8-di-*tert*-butyl-1,3-dioxo-1*H*-benzo[*de*]-isoquinolin-2(3*H*)-yl)acetamide) (Rotaxane 1). Following the general procedure, to a solution of thread **5** (0.460 g, 0.536 mmol) and Et_3N (1.81 mL, 12.8 mmol) in $CHCl_3$ were added simultaneously separate solutions of *p*-xylylene diamine (0.877 g, 6.44 mmol) and isophthaloyl dichloride (0.877 g, 6.44 mmol) in $CHCl_3$. Column chromatography (silica gel, CH_2Cl_2/acetone, 9:1) gave rotaxane **1** (0.052 g, 7%) as a white solid: ^{1}H NMR (400 MHz, $CDCl_3$) δ = 8.50 (s, 4H, H_b), 8.10 (bs, 10H, Hc+ H_B+ H_C), 7.91 (s, 4H, H_D), 7.51 (t, J = 8.1, 2H, H_A), 7.06 (s, 8H, H_F), 6.57 (s, 2H, H_e), 4.41 (s, 4H, H_d), 4.36 (d, J = 7.5, 8H, H_E), 2.68 (bs, 4H, H_f), 1.42 (s, 36H, H_a), 1.04−1.01 (m, 4H, H_g), 0.87−0.81 (m, 10H, alkyl chain); ^{13}C NMR (100 MHz, $CDCl_3$) δ = 167.0 (CO), 164.7 (CO), 150.4 (ArC), 137.4 (ArC), 134.3 (ArC), 132.1 (ArC), 131.2 (ArCH), 129.7 (ArCH), 129.2 (ArCH), 128.9 (ArCH), 128.9 (ArCH), 125.3 (ArC), 121.7 (ArC), 44.9 (CH_2), 42.7 (CH_2), 39.9 (CH_2), 35.4 (C_q), 31.3 (CH_3), 29.2 (CH_2), 29.1 (CH_2), 28.8 (CH_2), 26.7 (CH_2); FAB-MS (3-NOBA matrix) m/z = 1389.724 $[M + H]^+$ (Calcd for $C_{85}H_{96}N_8O_{10}$ + H^+ m/z = 1389.725). Calcd for $C_{85}H_{96}N_8O_{10}$: C 73.46, H 6.96, N 8.06. Found: C 73.28, H 7.06, N 8.00.

[2]-(1,4,7,14,17,20-Hexaaza-2,6,15,19-tetraoxo-3,5,9,12,16,18,22,25-tetrabenzocyclohexacosane)-*N*,*N*′-(heptacosane-1,27-diyl)bis(2-(5,8-di-*tert*-butyl-1,3-dioxo-1*H*-benzo-[*de*]isoquinolin-2(3*H*)-yl)acetamide) (Rotaxane 3). Following the general procedure, to a solution of thread **7** (0.364 g, 0.332 mmol) and Et_3N (1.21 mL, 8.63 mmol) in $CHCl_3$ were added simultaneously separate solutions of *p*-xylylene diamine (0.542 g, 3.98 mmol) and isophthaloyl dichloride (0.542 g, 3.98 mmol) in $CHCl_3$. Column chromatography (silica gel, CH_2Cl_2/acetone, 9:1) gave rotaxane **3** (0.038 g, 7%) as a white solid: mp = 164−165 °C; ^{1}H NMR (500 MHz, CD_2Cl_2) δ = 8.52 (d, J = 1.4, 4H, H_b), 8.20 (d, J = 1.7, 4H, H_c), 8.15 (s, 2H, H_C), 8.07 (dd, J = 7.8, J = 1.3, 4H, H_B), 7.88 (t, J = 4.9, 4H, H_D), 7.54 (s, 2H, H_A), 7.03 (s, 8H, H_F), 6.42 (bs, 2H, H_e), 4.39 (bs, 8H, H_E), 4.16 (bs, 4H, H_d), 2.89 (m, 4H, H_f), 1.49−1.45 (m, 40H, H_a+ H_g), 1.32−1.08 (m, 44H, CH_2 alkyl chain); ^{13}C NMR (100 MHz, $CDCl_3$) δ = 166.9 (CO), 166.5 (CO), 164.3(CO), 150.2 (ArC), 137.0 (ArC), 134.1 (ArC), 131.8 (ArC), 130.9 (ArCH), 129.7 (ArCH), 129.5 (ArCH), 128.9 (ArCH), 128.6 (ArCH), 125.0 (ArCH), 124.8 (ArC), 121.3 (ArC), 44.7 (CH_2), 42.2 (CH_2), 39.7 (CH_2), 35.1 (CH_2), 31.0 (CH_3), 29.5 (CH_2), 29.4 (CH_2), 29.3 (CH_2), 29.3 (CH_2), 29.2 (CH_2), 29.1 (CH_2), 28.9 (CH_2), 26.74 (CH_2); FAB-MS (3-NOBA matrix) m/z = 1627.990 $[M + H]^+$ (Calcd for $C_{102}H_{130}N_8O_{10}$ + H^+ m/z = 1627.991). Calcd for $C_{102}H_{130}N_8O_{10}$: C 75.24 H 8.05, N 6.88. Found: C 75.35, H 8.07 N 6.81.

[2]-(1,4,7,14,17,20-Hexaaza-2,6,15,19-tetraoxo-3,5,9,12,16,18,22,25-tetrabenzocyclohexacosane)-*N*,*N*′-((ethyne-1,2-diylbis(4,1-phenylene))bis(methylene))bis(2-(5,8-di-*tert*-butyl-1,3-dioxo-1*H*-benzo[de]isoquinolin-2(3*H*)-yl)-acetamide) (Rotaxane 4). Following the general procedure, to a solution of thread **8** (0.150 g, 0.160 mmol) and Et_3N (541 μL, 3.88 mmol) in $CHCl_3$ were added simultaneously separate solutions of *p*-xylylene diamine (0.261 g, 1.92 mmol) and isophthaloyl dichloride (0.261 g, 41.9 mmol) in $CHCl_3$. Column chromatography (silica gel, CH_2Cl_2/ MeOH, 97:3) gave rotaxane **2** (0.014 g, 6%) as a white solid: mp >315 °C; ^{1}H NMR (500 MHz, CD_2Cl_2) δ = 8.55 (d, J = 1.2 Hz, 4H, H_b), 8.20 (d, J = 1.2 Hz, 4H, H_c), 8.15 (d, J = 7.2 Hz, 4H, H_B), 8.14 (s, 2H, H_C), 7.85 (bs, 4H, H_D), 7.60 (t, J = 7.2 Hz, 2H, H_A), 7.40 (d, J = 8.0 Hz, 4H, H_h), 7.10 (d, J = 8.0 Hz, 4H, H_g), 6.90 (s, 8H, H_F), 6.66 (bs, 2H, H_e), 4.41 (bs, 8H, H_E), 4.24 (bs, 8H, H_d + H_f), 1.41 (s, 36H, H_a). The low solubility of rotaxane **4** did not allow the acquisition of ^{13}C spectra with sufficiently good signal/noise ratio. HRMS (FAB, 3-NOBA matrix) m/z = 1467.677 $[M + H]^+$ (Calcd for

dx.doi.org/10.1021/jo300907r | J. Org. Chem. 2012, 77, 5724−5735

$C_{92}H_{90}N_8O_{10}$ + H^+ m/z = 1467.678). Calcd for $C_{92}H_{90}N_8O_{10}$: C 75.28, H 6.18, N 7.63. Found: C 75.38, H 6.21, N 7.57.

***N,N′*-(Nonane-1,9-diyl)bis(2-(5,8-di-*tert*-butyl-1,3-dioxo-1*H*-benzo[*de*]isoquinolin-2(3*H*)-yl)acetamide) (Thread 5).** To a stirred solution of compound **9** (0.250 g, 0.680 mmol) in DMF (15 mL) under nitrogen was added BOP (0.361 g, 0.816 mmol) in one portion, and the reaction mixture was stirred at room temperature for 0.5 h. 1,9-Diaminononane **10** (0.076 g, 0.481 mmol) and DIPEA (8.29 μL, 4.76 mmol) were added sequentially, and the mixture was stirred overnight at room temperature. After removal of the solvent, the residue was redissolved in CH_2Cl_2 (100 mL), washed with H_2O (100 mL), dried over $MgSO_4$, and concentrated under reduced pressure. The crude product was purified by column chromatography on silica gel eluting with a gradient of CH_2Cl_2 and acetone (starting from 0 to 10% acetone). Compound **5** (0.268 g, 65%) was obtained as an oil, which was precipitated from CH_2Cl_2/*n*-pentane to obtain a white solid: ^{1}H NMR (400 MHz, $CDCl_3$) δ = 8.64 (d, J = 1.7, 4H, H_b), 8.13 (d, J = 1.7, 4H, H_c), 6.12 (d, J = 5.6, 2H, H_e), 4.82 (s, 4H, H_d), 3.25 (td, J = 6.8, J = 5.6, 4H, H_f), 1.52−1.46 (m, 40H, H_a+ H_g), 1.30−1.24 (m, 10H, alkyl chain); ^{13}C NMR (100 MHz, $CDCl_3$) δ = 166.9 (CO), 164.3 (CO), 163.3 (ArC), 131.9 (ArC), 129.5 (ArCH), 129.4 (ArCH), 124.8 (ArC), 121.5 (ArC), 42.8 (CH_2), 39.5(CH_2), 35.3 (CH_2), 35.1 (CH_2), 31.0 (CH_3), 29.2 (CH_2), 28.9 (CH_2), 28.7 (CH_2), 26.4 (CH_2); FAB-MS (3-NOBA matrix) m/z = 857.513 $[M + H]^+$ (Calcd for $C_{53}H_{68}N_4O_6$ + H^+ m/z = 857.514). Calcd for $C_{53}H_{68}N_4O_6$: C 74.27, H 8.00, N 6.54. Found: C 74.5, H 8.22, N 6.61.

***N,N′*-(Heptacosane-1,27-diyl)bis(2-(5,8-di-*tert*-butyl-1,3-dioxo-1*H*-benzo[*de*]isoquinolin-2(3*H*)-yl)acetamide) (Thread 7).** Procedure as for thread **5**, coupling reaction of **9** (0.340 g, 0.962 mmol) with 1,26-diaminohexacosane **12** (0.174 g, 0.423 mmol) gave thread **7** as a white solid (0.278 g, 60%): mp = 127−128 °C; ^{1}H NMR (400 MHz, $CDCl_3$) δ = 8.68 (d, J = 1.8, 4H, H_b), 8.16 (d, J = 1.8, 4H, H_c), 5.79 (t, J = 5.6, 2H, H_e), 4.87 (s, 4H, H_d), 3.31 (td, J = 6.8, 5.6, 4H), 1.49 (s, 40H, H_a and H_g), 1.29−1.25 (m, 44H, alkyl chain); ^{13}C NMR (100 MHz, $CDCl_3$) δ = 166.8 (CO), 164.3 (CO), 150.1 (ArC), 131.9 (ArC), 129.6 (ArCH), 129.4 (ArCH), 124.9 (ArC), 121.5 (ArC), 43.0 (CH_2), 39.7 (CH_2), 35.1 (C_q), 31.0 (CH_3), 29.5 (CH_2), 29.5(CH_2), 29.4 (CH_2), 29.4(CH_2), 29.3(CH_2), 29.2 (CH_2), 29.1 (CH_2), 26.7 (CH_2); FAB-MS (3-NOBA matrix) m/z = 1095.781 $[M + H]^+$ (Calcd for $C_{70}H_{102}N_4O_6$ + H^+ m/z = 1095.780). Calcd for $C_{70}H_{102}N_4O_6$: 76.74, H 9.38, N 5.11. Found: C 76.48, H 9.32, N 5.01.

***N,N′*-((Ethyne-1,2-diylbis(4,1-phenylene))bis(methylene))-bis(2-(5,8-di-*tert*-butyl-1,3-dioxo-1*H*-benzo[*de*]isoquinolin-2(3*H*)-yl)acetamide) (Thread 8).** Procedure as for thread **5**, coupling reaction of **9** (0.408 g, 1.15 mmol) with compound **18** (0.125 g, 0.529 mmol) gave thread **8** as a yellow solid (0.401 g, 90%): mp = 216−217 °C; ^{1}H NMR (400 MHz, $CDCl_3$) δ = 8.69 (d, J = 1.8, 4H, H_b), 8.17 (d, J = 1.8, 4H, H_c), 7.50 (d, J = 8.0, 4H, H_h), 7.31 (d, J = 8.0, 4H, H_g), 6.12 (t, J = 5.8, 1H, H_e), 4.96 (s, 4H, H_d), 4.54 (d, J = 5.8, 4H, H_f), 1.50 (s, 36H, H_a); ^{13}C NMR (100 MHz, DMSO-d_6) δ = 167.0 (CO), 163.6 (CO), 149.7 (ArC), 140.1 (ArC),131.8 (ArC), 131.3 (ArCH), 129.9 (ArCH), 128.2 (ArCH), 127.4 (ArCH), 124.4 (ArC), 121.6 (ArC), 120.7 (ArC), 89.4 (C≡C), 42.6 (CH_2), 41.9 (CH_2), 35.0 (C_q), 30.9 (CH_3). HRMS (FAB, 3-NOBA matrix) m/z = 935.466 $[M + H]^+$ (anal. Calcd for $C_{60}H_{62}N_4O_6$ + H^+ m/z = 935.467). Calcd for $C_{60}H_{62}N_4O_6$: C 77.06, H 6.68, N 5.99. Found: C 77.16, H 6.60, N 5.82.

***tert*-Butyl 4-Iodobenzylcarbamate (14).** Compound **14** was prepared using a modification of the literature procedure.[46] A solution of 4-iodobenzylamine hydrochloride **13** (0.400 g, 1.48 mmol) in THF (30 mL) was treated with Et_3N (1.49 g, 14.8 mmol) and di-*tert*-butyl dicarbonate (0.647 g, 2.96 mmol). After the reaction mixture was stirred overnight at room temperature, THF was removed under reduced pressure. The residue was dissolved in hexane and purified by flash column chromatography on silica gel with EtOAc/hexanes (1:3) as eluent to afford *tert*-butyl 4-iodobenzylcarbamate **8**. After crystallization from hexane, the title compound **8** (0.370 g, 75%) was obtained as a white solid: mp = 91−93 °C; ^{1}H NMR ($CDCl_3$) δ = 7.65 (d, J = 8.4, 2H, ArCH), 7.03 (d, J = 8.4 Hz, 2H, ArCH), 4.88 (bs, 1H, NH), 4.33 (d, J = 5.6, 2H, NH), 1.47 (s, 9H, CH_3).

***tert*-Butyl 4-((Trimethylsilyl)ethynyl)benzylcarbamate (15).** Following a general Pd-coupling procedure, a solution of *tert*-butyl-4-iodobenzylcarbamate (0.250 g, 0.750 mmol) **14** in THF (25 mL) was treated with (trimethylsilyl)acetylene (127 μL, 0.900 mmol), Et_3N (211 μL, 0.150 mmol), CuI (14.3 mg, 0.0750 mmol), and $(PPh_3)Pd_2Cl_2$ (26.3 mg, 0.0375 mmol) and stirred at 50 °C for 2 h. The reaction mixture was diluted with Et_2O, filtered through Celite, and evaporated to dryness. The residue was purified by flash column chromatography on silica gel with EtOAc/hexane (1:10). Then the obtained solid was recrystallized from *n*-hexane to afford **15** as a yellow solid: mp = 95−96 °C; ^{1}H NMR ($CDCl_3$) δ = 7.66 (d, J = 7.9, 2H, ArCH), 7.05 (d, J = 7.9, 2H, ArCH), 4.86 (bs, 1H, NH), 4.23 (d, J = 5.2, 2H, CH_2), 1.47 (s, 9H, CH_3), 0.260 (s, 9H, CH_3).

Di-*tert*-butyl ((Ethyne-1,2-diylbis(4,1-phenylene))bis-(methylene))dicarbamate (17). Following a general Pd-coupling procedure, a solution of *tert*-butyl-4-iodobenzylcarbamate **14** (0.106 g, 0.458 mmol) in toluene (10 mL) was treated with *tert*-butyl-4-ethynylbenzylcarbamate **16** (0.198 g, 0.596 mmol),[46] Et_3N (2.00 mL, 14.2 mmol), CuI (8.73 mg, 0.045 mmol), and $(PPh_3)Pd_2Cl_2$ (22.5 mg, 0.032 mmol) and stirred at 60 °C for 24 h. After cooling down to room temperature, the reaction mixture was filtered through a pad of Celite, and the solvent was removed under reduced pressure. The residue was purified by column chromatography (SiO_2, hexane/EtOAc 5:1) to give compound **17** as a yellow solid: ^{1}H NMR (400 MHz, $CDCl_3$) δ = 7.51 (d, J = 8.0, 4H, ArCH), 7.28 (d, J = 8.0, 4H, ArCH), 4.87 (bs, 2H, NH), 4.35 (d, J = 5.2, 4H, CH_2), 1.49 (s, 18H, CH_3); ^{13}C NMR (100 MHz, $CDCl_3$) δ = 156.0 (CO), 139.3 (ArC), 132.0 (ArCH), 127.5 (ArCH), 122.3 (ArC), 89.3 (C≡C), 44.5 (CH_2), 31.7 (C_q), 28.5 (CH_3); UV−vis ($CHCl_3$) λ_{max} (nm) = 273, 289, 297, 307; Fluorescence ($CHCl_3$) λ (nm) = 311, 324, 331.

(Ethyne-1,2-diylbis(4,1-phenylene))dimethanamine (18). A cooled solution of compound **17** (0.100 g, 0.229 mmol) in anhydrous CH_2Cl_2 (5 mL) at 0 °C was treated with TFA (1 mL). After the reaction mixture was stirred at room temperature for 1 h, the solvent was evaporated. The residue was diluted with CH_2Cl_2 and concentrated under reduced pressure several times to afford **18** (0.053 g, 98%) as a white solid: mp = 202−204 °C; ^{1}H NMR (400 MHz, MeOD) δ = 7.62 (d, J = 8.2, 4H, ArCH), 7.50 (d, J = 8.2, 4H, ArCH), 4.16 (bs, 4H, CH_2); ^{13}C NMR (100 MHz, MeOD) δ = 134.9 (ArC), 133.2 (ArCH), 130.2 (ArCH), 125.1 (ArC), 90.3 (C≡C), 44.0 (CH_2); FAB-MS (3-NOBA matrix) m/z = 237.132 $[M + H]^+$ (Calcd for $C_{16}H_{16}N_2$ + H^+ m/z = 237.131).

■ ASSOCIATED CONTENT

Ⓢ Supporting Information

^{1}H and ^{13}C spectra of intermediate compounds and variable temperature ^{1}H NMR spectra of rotaxane **1**. This material is available free of charge via the Internet at http://pubs.acs.org.

■ AUTHOR INFORMATION

Corresponding Author

*E-mail: A.M.Brouwer@uva.nl.

Notes

The authors declare no competing financial interest.

■ ACKNOWLEDGMENTS

This work was supported by NanoNed, a national nanotechnology program coordinated by the Dutch Ministry of Economic Affairs. The authors thank Dr. Bert Bakker for the synthesis of 1,26-diaminohexacosane **12**.

■ REFERENCES

(1) Bissell, R. A.; Córdova, E.; Kaifer, A. E.; Stoddart, J. F. *Nature* **1994**, *369*, 133−137.

(2) Lane, A. S.; Leigh, D. A.; Murphy, A. *J. Am. Chem. Soc.* **1997**, *119*, 11092−11093.

(3) Bermudez, V.; Capron, N.; Gase, T.; Gatti, F. G.; Kajzar, F.; Leigh, D. A.; Zerbetto, F.; Zhang, S. W. *Nature* **2000**, *406*, 608−611.
(4) Leigh, D. A.; Troisi, A.; Zerbetto, F. *Angew. Chem., Int. Ed.* **2000**, *39*, 350−353.
(5) Zhao, X.; Jiang, X. K.; Shi, M.; Yu, Y. H.; Xia, W.; Li, Z. T. *J. Org. Chem.* **2001**, *66*, 7035−7043.
(6) Sauvage, J. P.; Dietrich-Buchecker, C. *Molecular Catenanes, Rotaxanes and Knots*; VCH-Wiley: Weinheim, 1999.
(7) Jeppesen, J. O.; Perkins, J.; Becher, J.; Stoddart, J. F. *Angew. Chem., Int. Ed.* **2001**, *40*, 1216−1221.
(8) Brouwer, A. M.; Frochot, C.; Gatti, F.; Leigh, D. A.; Mottier, L.; Paolucci, F.; Roffia, S.; Wurpel, G. W. H. *Science* **2001**, *291*, 2124−2128.
(9) Wurpel, G. W. H.; Brouwer, A. M.; van Stokkum, I. H. M.; Farran, M. A.; Leigh, D. A. *J. Am. Chem. Soc.* **2001**, *123*, 11327−11328.
(10) Marlin, D. S.; Cabrera, D. G.; Leigh, D. A.; Slawin, A. M. Z. *Angew. Chem., Int. Ed.* **2006**, *45*, 77−83.
(11) Aprahamian, I.; Dichtel, W.; Ikeda, T.; Heath, J.; Stoddart, J. F. *Org. Lett.* **2007**, *9*, 1287−1290.
(12) Baggerman, J.; Jagesar, D. C.; Valleé, R. A. L.; Hofkens, J.; De Schryver, F. C.; Schelhase, F.; Vögtle, F.; Brouwer, A. M. *Chem.—Eur. J.* **2007**, *13*, 1291−1299.
(13) Durola, F.; Lux, J.; Sauvage, J.-P. *Chem.—Eur. J.* **2009**, *15*, 4124−4134.
(14) Gassensmith, J. J.; Baumes, J. M.; Smith, B. D. *Chem. Commun.* **2009**, 6329−6338.
(15) Johnson, J. R.; Fu, N.; Arunkumar, E.; Leevy, W. M.; Gammon, S. T.; Piwnica-Worms, D.; Smith, B. D. *Angew. Chem., Int. Ed.* **2007**, *46*, 5528−5531.
(16) Berná, J.; Alajarín, M.; Orenes, R.-A. *J. Am. Chem. Soc.* **2010**, *132*, 10741−10747.
(17) Feringa, B. L. *Molecular Switches*, 2nd ed.; Wiley-VCH: Weinheim, 2001.
(18) Browne, W. R.; Feringa, B. L. *Nat. Nanotechnol.* **2006**, *1*, 25−35.
(19) Gust, D.; Moore, T. A.; Moore, A. L. *Chem. Commun.* **2006**, 1169−1178.
(20) Balzani, V.; Credi, A.; Raymo, F. M.; Stoddart, J. F. *Angew. Chem., Int. Ed.* **2000**, *39*, 3349−3391.
(21) Balzani, V.; Credi, A.; Venturi, M. *Molecular Devices and Machines—Concepts and Perspectives for the Nanoworld*; Wiley-VCH: Weinheim, 2008.
(22) Balzani, V.; Clemente-Leon, M.; Credi, A.; Ferrer, B.; Venturi, M.; Flood, A. H.; Stoddart, J. F. *Proc. Natl. Acad. Sci. U. S. A.* **2006**, *103*, 1178−1183.
(23) Astumian, R. D. *Phys. Chem. Chem. Phys.* **2007**, *9*, 5067−5083.
(24) Harada, A. *Acc. Chem. Res.* **2001**, *34*, 456−464.
(25) Hirose, K.; Shiba, Y.; Ishibashi, K.; Doi, Y.; Tobe, Y. *Chem.—Eur. J.* **2008**, *14*, 3427−3433.
(26) Kay, E. R.; Leigh, D. A.; Zerbetto, F. *Angew. Chem., Int. Ed.* **2007**, *46*, 72−191.
(27) Tian, H.; Wang, Q. C. *Chem. Soc. Rev.* **2006**, *35*, 361−374.
(28) Collin, J. P.; Dietrich-Buchecker, C.; Gaviña, P.; Jimenez-Molero, M. C.; Sauvage, J. P. *Acc. Chem. Res.* **2001**, *34*, 477−487.
(29) Moretto, A.; Menegazzo, I.; Crisma, M.; Shotton, E. J.; Nowell, H.; Mammi, S.; Toniolo, C. *Angew. Chem., Int. Ed.* **2009**, *48*, 8986−8989.
(30) Aprahamian, I.; Yasuda, T.; Ikeda, T.; Saha, S.; Dichtel, W. R.; Isoda, K.; Kato, T.; Stoddart, J. F. *Angew. Chem., Int. Ed.* **2007**, *46*, 4675−4679.
(31) Busseron, E.; Romuald, C.; Coutrot, F. *Chem.—Eur. J.* **2010**, *16*, 10062−10073.
(32) Olsen, J. C.; Fahrenbach, A. C.; Trabolsi, A.; Friedman, D. C.; Dey, S. K.; Gothard, C. M.; Shveyd, A. K.; Gasa, T. B.; Spruell, J. M.; Olson, M. A.; Wang, C.; de Rouville, H. P. J.; Botros, Y. Y.; Stoddart, J. F. *Org. Biomol. Chem.* **2011**, *9*, 7126−7133.
(33) You, Y.-C.; Tzeng, M.-C.; Lai, C.-C.; Chiu, S.-H. *Org. Lett.* **2012**, *14*, 1046−1049.
(34) Panman, M. R.; Bodis, P.; Shaw, D. J.; Bakker, B. H.; Newton, A. C.; Kay, E. R.; Leigh, D. A.; Buma, W. J.; Brouwer, A. M.; Woutersen, S. *Phys. Chem. Chem. Phys.* **2012**, *14*, 1865−1875.
(35) Panman, M. R.; Bodis, P.; Shaw, D. J.; Bakker, B. H.; Newton, A. C.; Kay, E. R.; Brouwer, A. M.; Buma, W. J.; Leigh, D. A.; Woutersen, S. *Science* **2010**, *328*, 1255−1258.
(36) Jagesar, D. C.; Fazio, S. M.; Taybi, J.; Eiser, E.; Gatti, F.; Leigh, D. A.; Brouwer, A. M. *Adv. Funct. Mater.* **2009**, *19*, 3440−3449.
(37) Altoè, P.; Haraszkiewicz, N.; Gatti, F. G.; Wiering, P. G.; Frochot, C.; Brouwer, A. M.; Balkowski, G.; Shaw, D.; Woutersen, S.; Buma, W. J.; Zerbetto, F.; Orlandi, G.; Leigh, D. A.; Garavelli, M. *J. Am. Chem. Soc.* **2009**, *131*, 104−117.
(38) Jagesar, D. C.; Hartl, F.; Buma, W. J.; Brouwer, A. M. *Chem.—Eur. J.* **2008**, *14*, 1935−1946.
(39) Gatti, F. G.; León, S.; Wong, J. K. Y.; Bottari, G.; Altieri, A.; Morales, A. M. F.; Teat, S. J.; Frochot, C.; Leigh, D. A.; Brouwer, A. M.; Zerbetto, F. *Proc. Natl. Acad. Sci. U. S. A.* **2003**, *100*, 10−14.
(40) Murgu, I.; Baumes, J. M.; Eberhard, J.; Gassensmith, J. J.; Arunkumar, E.; Smith, B. D. *J. Org. Chem.* **2011**, *76*, 688−691.
(41) Gatti, F. G.; Leigh, D. A.; Nepogodiev, S. A.; Slawin, A. M. Z.; Teat, S. J.; Wong, J. K. Y. *J. Am. Chem. Soc.* **2001**, *123*, 5983−5989.
(42) Günbaş, D. D.; Zalewski, L.; Brouwer, A. M. *Chem. Commun.* **2010**, *46*, 2061−2063.
(43) Ghosh, P.; Federwisch, G.; Kogej, M.; Schalley, C. A.; Haase, D.; Saak, W.; Lützen, A.; Gschwind, R. M. *Org. Biomol. Chem.* **2005**, *3*, 2691−2700.
(44) Yoon, I. L.; Benitez, D.; Zhao, Y.-L.; Miljanic, O. S.; Kim, S.-Y.; Tkatchouk, E.; Leung, K. C. F.; Khan, S. I.; Goddard, W. A.; Stoddart, J. F. *Chem.—Eur. J.* **2009**, *15*, 1115−1122.
(45) Li, H.; Zhao, Y.-L.; Fahrenbach, A. C.; Kim, S.-Y.; Paxton, W. F.; Stoddart, J. F. *Org. Biomol. Chem.* **2011**, *9*, 2240−2250.
(46) Lee, J.; Kang, S.; Lim, J.; Choi, H.; Jin, M.; Toth, A.; Pearce, L.; Tran, R.; Wang, Y.; Szabo, T.; Blumberg, P. *Bioorg. Med. Chem.* **2004**, *12*, 371−385.
(47) Tanev, P. T.; Liang, Y.; Pinnavaia, T. J. *J. Am. Chem. Soc.* **1997**, *119*, 8616−8624.
(48) Bottari, G.; Dehez, F.; Leigh, D. A.; Nash, P. J.; Pérez, E. M.; Wong, J. K. Y.; Zerbetto, F. *Angew. Chem., Int. Ed.* **2003**, *42*, 5886−5889.
(49) Leigh, D. A.; Morales, M. Á. F.; Pérez, E. M.; Wong, J. K. Y.; Slawin, A. M. Z.; Carmichael, A. J.; Haddleton, D. M.; Brouwer, A. M.; Buma, W. J.; Wurpel, G. W. H.; León, S.; Zerbetto, F. *Angew. Chem., Int. Ed.* **2005**, *44*, 3062−3067.
(50) Nygaard, S.; Leung, K. C. F.; Aprahamian, I.; Ikeda, T.; Saha, S.; Laursen, B. W.; Kim, S.-Y.; Hansen, S. W.; Stein, P. C.; Flood, A. H.; Stoddart, J. F.; Jeppesen, J. O. *J. Am. Chem. Soc.* **2007**, *129*, 960−970.
(51) Jeppesen, J. O.; Vignon, S. A.; Stoddart, J. F. *Chem.—Eur. J.* **2003**, *9*, 4611−4625.
(52) Liu, Y.; Flood, A. H.; Bonvallett, P. A.; Vignon, S. A.; Northrop, B. H.; Tseng, H. R.; Jeppesen, J. O.; Huang, T. J.; Brough, B.; Baller, M.; Magonov, S.; Solares, S. D.; Goddard, W. A.; Ho, C. M.; Stoddart, J. F. *J. Am. Chem. Soc.* **2005**, *127*, 9745−9759.
(53) Harris, R. K. *Nuclear Magnetic Resonance Spectroscopy*; Longman Scientific & Technical: Essex, U.K., 1986.
(54) Gutowsky, H. S.; Holm, C. H. *J. Chem. Phys.* **1956**, *25*, 1228−1234.
(55) Stephenson, D. S.; Binsch, G. *J. Magn. Reson.* **1969**, *32*, 145−152.
(56) Mancini, G.; Zazza, C.; Aschi, M.; Sanna, N. *Phys. Chem. Chem. Phys.* **2011**, *13*, 2342−2349.
(57) Li, H.; Jiang, Z.; Wang, X.; Zheng, C. *Synth. Commun.* **2006**, *36*, 1933−1940.